Unexpected Ultrafast Silver Ion Reduction: Dynamics Driven by the Solvent Structure

8 **AUTHORS**, INCLUDING:

Anna Balcerzyk
Université Paris-Sud 11
8 PUBLICATIONS   61 CITATIONS

SEE PROFILE

Uli Schmidhammer
Université Paris-Sud 11
54 PUBLICATIONS   516 CITATIONS

SEE PROFILE

Simon Martin Pimblott
The University of Manchester
105 PUBLICATIONS   2,066 CITATIONS

SEE PROFILE

Mehran Mostafavi
Université Paris-Sud 11
162 PUBLICATIONS   2,910 CITATIONS

SEE PROFILE

Unexpected Ultrafast Silver Ion Reduction: Dynamics Driven by the Solvent Structure

Anna Balcerzyk,[†] Uli Schmidhammer,[†] Gregory Horne,[†,‡,§] Furong Wang,[†] Jun Ma,[†] Simon M. Pimblott,[‡,§] Aurélien de la Lande,[†] and Mehran Mostafavi*,[†]

[†]Laboratoire de Chimie Physique, CNRS/Université Paris-Sud, Bâtiment 349, 91405 Orsay, France

[‡]Dalton Cumbrian Facility, The University of Manchester, Westlakes Science and Technology Park, Moor Row, Cumbria, CA24 3HA, United Kingdom

[§]School of Chemistry, The University of Manchester, Oxford Road, Manchester M13 9PL, United Kingdom

Ⓢ *Supporting Information*

ABSTRACT: Picosecond pulse radiolysis measurements have been performed in neutral and highly acidic aqueous solutions containing silver ions at different concentrations. Silver ion reduction is used to understand the ultrafast chemistry of irradiated water and aqueous solutions. The absorption band measured at the end of the 7-ps electron pulses has an intense band with a maximum at 360 nm due to the formation of silver atoms. Kinetics shows that the amount of silver atom formed at the end of the electron pulse in phosphoric acid solutions is greater than that in neutral water. This unexpectedly high yield of silver atom formation cannot be explained solely by the reaction between silver ions and solvated electrons in neutral solutions nor by the reaction with hydrogen atoms in phosphoric acid solutions. To explain the observed ultrafast reduction of silver ions, the presolvated electron, be it free or paired to the hydronium cation, must react very quickly with a silver ion, potentially competing with geminate recombination of the electron and its sibling radical cation.
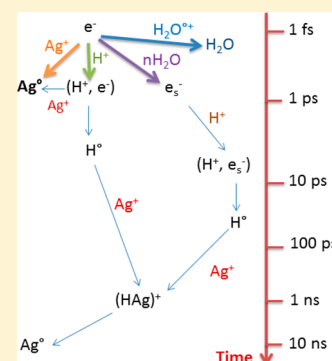
INTRODUCTION

The reactivity of presolvated electrons and solvated electrons (e^- and e_s^-, respectively), as well as hydrogen atoms ($H^{\bullet}$), is crucially important in determining reducing chemistry during water radiolysis. In pure water and diluted aqueous solutions, presolvated electrons are produced via reaction 1 (Table 1), and subsequently undergo a number of ultrafast processes, such as solvation (Table 1 reaction 2) and geminate recombination with the water cation ($H_2O^{\bullet+}$) (Table 1 reaction 3), in less than 1 ps. Thanks to its intense absorption band, reduction reactions involving the solvated electron can be followed in the subnanosecond time regime, using ultrafast pump−probe measurement techniques. However, scavengers (added solutes) are typically used to estimate the reactivity of the presolvated electron and hydrogen atom.

Formation of the silver atoms by reacting silver ions with hydrated electrons and hydrogen atoms has been studied using pulse radiolysis techniques since the 1970s.[1−3] The intense absorption band of the silver atom, and the relative simplicity of using a monovalent redox system, allowed the facile determination of the step-by-step formation kinetics of silver atom clusters from silver ions.[4−10] These investigations demonstrated that the silver atom exhibits a redox potential lower than that of bulk metal silver.[11,12] The reduction of silver ions has also been studied using several chemical reducing agents, although it is now clear that at room temperature such reactions can only occur when silver ions are adsorbed on pre-existing nuclei or impurities as a consequence of the low redox potential of the silver atom.

The reduction of the silver ion by the hydrated electron (Table 1 reaction 5) has been investigated by a number of groups, and a diffusion-controlled rate constant of around 4×10^{10} M^{-1} s^{-1} has been determined.[13] In contrast, the reaction of the silver ion with $H^{\bullet}$ is not diffusion controlled, possessing a rate constant of 2×10^{10} M^{-1} s^{-1}.[13] It has been proposed that the reduction of silver ion by $H^{\bullet}$ involves the formation of a complex atom ($AgH^{\bullet+}$), through reaction 6 (Table 1), which subsequently reduces the silver ion via reaction 7.[14] Additionally, the oxidation of silver ion by $OH^{\bullet}$ through reactions 8 and 9 (Table 1) has also been carefully studied.

The straightforward chemistry and the intense absorption band of the silver atom suggest that silver atom formation can be used to follow the dynamics of electron transfer in ultrafast processes. During the 1970s, Hunt and colleagues used a stereoscopic pulse radiolysis system with a time resolution of around 30 ps to show that in aqueous solution of sufficiently high concentration a large number of scavengers, apart from the hydronium cation, decrease the initial yield of the hydrated electron. They determined the concentrations of a number of neutral and charged solutes for which the initial concentration of the hydrated electron is reduced by 63%, C_{37}.[15] Later, Jonah

Table 1. Elementary Reactions Involved in Pulse Radiolysis of Aqueous Solutions of Neutral and Concentrated Phosphoric Acid Containing Silver Ions

$H_2O \rightarrow H_2O^{\bullet+} + e^-$	1
$e^- \rightarrow e_s^-$	2
$H_2O^{\bullet+} + e^- \rightarrow H_2O$	3
$H_2O + H_2O^{\bullet+} \rightarrow H_3O^+ + OH^\bullet$	4
$e_s^- + Ag^+ \rightarrow Ag^\circ$	5
$H^\bullet + Ag^+ \rightarrow AgH^{\bullet+}$	6
$AgH^{\bullet+} \rightarrow Ag^\circ + H^+$	7
$Ag^+ + OH^\bullet \rightarrow AgOH^+$	8
$AgOH^+ + H^+ \rightarrow Ag^{2+} + H_2O$	9
$e^- + Ag^+ \rightarrow Ag^\circ$	10
$e^- + H_3O^+ \rightarrow (H_3O^+, e^-)$	11
$(H_3O^+ + e^-) \rightarrow H_2O + H^\bullet$	12
$(H_3O^+ + e^-) + Ag^+ \rightarrow Ag^\circ + H_2O$	13
$H_3PO_4 \rightarrow H_2PO_4^\bullet + e^- + H^+$	14
$H_2O^{\bullet+} + H_3PO_4 \rightarrow H_2PO_4^\bullet + H_3O^+$	15

et al. performed supplementary measurements and presented a more precise analysis taking into account the time-dependent rate constant of the scavenger reaction with the solvated electron.[16] These studies showed that the scavenging of presolvated electron by silver ion through reaction 10 (Table 1) occurs with a C_{37} value of around 0.17 mol L^{-1}. Stochastic diffusion kinetics simulations also suggest that the precursor of hydrated electron is involved in total yield of reduction.[17]

In the present work, the dynamics of the reduction of monovalent silver ion is observed in neutral and acidic solutions. Picosecond pulse radiolysis measurements (pulse width ~7 ps) of ten solutions with concentrations ranging from 10 to 150 mM of silver ions were performed. The experiments were performed in neutral water and highly acidic phosphoric acid solution. Both the decay of the solvated electron and the formation of silver atom were measured by the pump−probe method to determine the yield of silver atom formation within the electron pulse at different concentrations of silver ion. Simulations of the track kinetics were performed for the neutral solutions and included the reaction between hydrated electron and silver ion. Finally, by comparing the yields of silver atom formed at short time, the role of the solvent structure in the

reduction reaction of silver ions is discussed and an explanation for the ultrafast reaction of silver ion in acidic medium is given.

EXPERIMENTAL SECTION

The picosecond pulse radiolysis transient absorbance measurements were performed at the electron facility ELYSE.[18,19] The transient absorption pulse−probe setup is based on the laser-electron intrinsic synchronization resulting from the laser-triggered photocathode of the accelerator. The main part of the femtosecond Ti:sapphire laser output is frequency tripled and used to produce the electron pulse that is accelerated by the RF fields. A part of the laser source is split off to generate an optical probe pulse that can be delayed relative to the electron bunch by a mechanical translation stage. For the present study, a broadband probe detection scheme was used, the principle of which has already been described in ref 20. A supercontinuum, generated by focusing ~1 μJ of the laser source into a 6-mm-thick CaF$_2$ disk, was used as the optical probe covering a wavelength range from the visible to the ultraviolet. A reference signal is split off from the broadband probe before the fused silica optical flow cell (FSOFC). Probe and reference beams were each coupled into an optical fiber, transmitted to a spectrometer, and dispersed onto a CCD. The combination of the broadband probe and the multichannel detector allows for the entire transient spectra to be recorded, independently of the shot-to-shot fluctuations and possible long-term drifts of the electron source.

All measurements were made in a FSOFC with a 5-mm optical path collinear to the electron pulse propagation. The electron pulses were of ~4 nC, with an electron energy of 6−8 MeV, delivered at repetition frequency of 10 Hz. The measurements were performed at 22.5 °C. The chemical compounds were purchased from Sigma-Aldrich and used without further purification. Water for dilution was purified by passage through a Millipore purification system.

RESULTS

Ten different aqueous solutions of silver perchlorate were studied by observing the decay kinetics and absorption spectra at the end of the electron pulse. The composition and properties of each solution are reported in Table 2.

The decay kinetics of the solvated electron at 700 nm and the silver atom at 370 nm were recorded for neutral aqueous solutions (Samples 1−5) as a function of silver ion concentration (0.01−0.15 mol L^{-1}) and are shown in Figure 1. The kinetics of the solvated electron (Figure 1, left panel) clearly show that an increase in silver ion concentration leads to a decrease in the initial amplitude of the absorbance of the

Table 2. Chemical Composition of the Samples Studied and their Density, ρ, Viscosity, η, and Electron Density, F

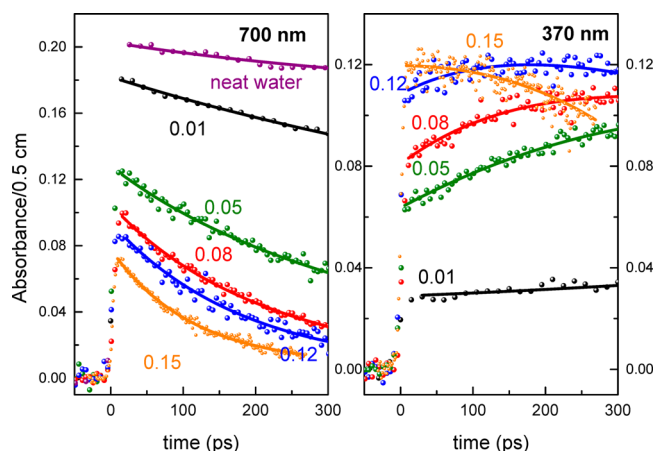| sample	acid concentration (mol L^{-1})	(Ag$^+$) (mol L^{-1})	H$_2$O (mol L^{-1})	ρ (g cm^{-3})	η (cP)	F	yield of Ag$^\circ$ at end of 7-ps pulse (10^7 mol J^{-1})
1	0	0.01	≈ 55.5	≈ 1	≈ 1	≈ 1	0.24
2	0	0.05	≈ 55.5	≈ 1	≈ 1	≈ 1	1.50
3	0	0.08	≈ 55.5	≈ 1	≈ 1	≈ 1	2.1
4	0	0.12	≈ 55.5	≈ 1	≈ 1	≈ 1	2.8
5	0	0.15	≈ 55.5	≈ 1	≈ 1	≈ 1	2.9
6	14.6/H$_3$PO$_4$	0.01	14.1	1.68	48.40	1.57	0.47
7	14.6/H$_3$PO$_4$	0.05	14.1	1.68	48.40	1.57	1.68
8	14.6/H$_3$PO$_4$	0.08	14.1	1.68	48.40	1.57	2.4
9	14.6/H$_3$PO$_4$	0.1	14.1	1.68	48.40	1.57	2.5
10	14.6/H$_3$PO$_4$	0.12	14.1	1.68	48.40	1.57	2.8

Figure 1. Kinetics observed at 700 (left) and 370 nm (right) for neat water and neutral solutions (samples 1−5) containing different concentrations of silver ion.

solvated electron. This decrease indicates that the precursor of the solvated electron is scavenged within the electron pulse. The absorption spectrum recorded at the end of the pulse has two maxima, one attributed to the solvated electron that is not totally scavenged after 7 ps and a second at 370 nm that is due to the silver atom (Figure 2, Top). The maximum absorption of
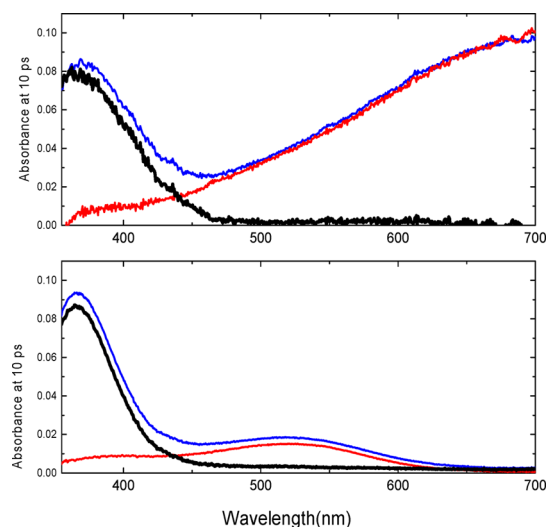

Figure 2. Top: Absorption spectra measured (blue) after 7-ps electron pulse in solution containing 0.08 mol L^{-1}Ag$^+$ in water. The measured spectrum is the superposition of the absorption of hydrated electron (red) and of silver atom (black). Bottom: Spectra in solutions containing 0.08 mol L^{-1} Ag$^+$ in 14.6 mol L^{-1} H$_3$PO$_4$. The measured spectrum is the superposition of the absorption of phosphate radical (red)[25] and of silver atom (black). Contribution of phosphate radical was subtracted from entire spectral region.

silver atom is located at 360 nm and the extinction coefficient at 370 nm is 14 500 M cm^{-1}.[21] The amount of silver atom formed within the electron pulse increases with the concentration of silver ion. At a silver ion concentration of 0.12 mol L^{-1}, the yield of silver atom formed within the electron pulse is 2.8 × 10^{-7} mol J^{-1}, which is very high. At higher silver ion concentrations, a slow decay is observed after the formation of silver atom which is attributed to the reaction of the silver atom with a silver ion, giving Ag$_2^+$. These data were used to

calculate the experimental yield of the solvated electron and silver atom at the end of the pulse which is presented in Table 2.

In neutral solution, the presolvated electron reacts rapidly with silver ion to yield silver atom. The C$_{37}$ value deduced from the measured decay kinetics is 0.14 mol L^{-1} (Figure S1 in the Supporting Information (SI)), which is close to that reported in the literature.[15,16] With the experimental data that gives access to both the solvated electron and silver atom signals, it is possible to estimate the sum of the yield of the solvated electron and that of the silver atom at the end of pulse. This total yield increases slightly from (4.2 ± 0.2) × 10^{-7} to (4.5 ± 0.2) × 10^{-7} mol J^{-1} when the concentration of silver ion is increased from 0.01 to 0.15 mol L^{-1}, respectively. Furthermore, the yield of presolvated electron available for the reduction reaction is higher than that of the hydrated electron, estimated to be around 4.5 × 10^{-7} mol J^{-1}, according to the stochastic simulations. The slight increase in the total yield suggests that reaction 10 and reaction 11 are in competition. It also indicates that in the presence of a moderate concentration of silver ion, the scavenging of free electrons by silver ion is not only in competition with the hydration process (reaction 2) but also with geminate recombination, which occurs within a few tens of femtoseconds as implied by the analysis reported in ref 22.

The track chemistry simulations performed in this work utilize a stochastic treatment of the radiation track structure and the independent reaction times modeling of the diffusion-reaction kinetics. A detailed description of this modeling methodology can be found in Pimblott and LaVerne.[23] Fast electron radiolysis track simulations were performed for aqueous silver perchlorate solutions to a time of 10 ps, with the number of realizations per permutation being at least 10^4. The dependence of the radiolytic yield of silver atom (Ag°) and e$_s^-$ as a function of AgClO$_4$ concentration are given in Figure 3 and compared to the experimental results.
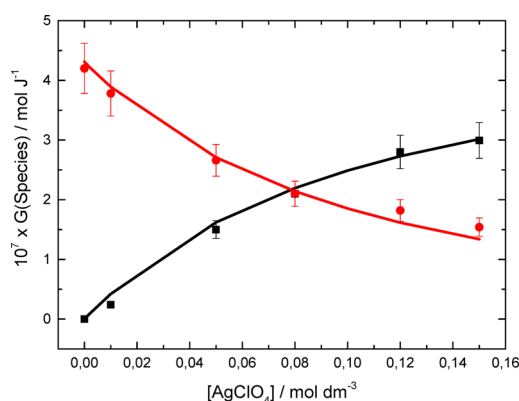

Figure 3. Radiolytic yield of Ag° and e$_{aq}^-$ as a function of AgClO$_4$ concentration at 10 ps; G(Ag°)$_{Experiment}$ (black square ■), G(Ag°)$_{Calculation}$ (black line —), G(e$_{aq}^-$)$_{Experiment}$ (red dot ●), G(e$_{aq}^-$)$_{Calculation}$ (red line —)).

The concentration dependence of Ag° and e$_s^-$ within 10 ps is in very good agreement with the experimental results and can be summarized as follows. As [AgClO$_4$] increases from 0 to 0.15 mol L^{-1}: (1) G(Ag°) increases with increasing [AgClO$_4$]; going from 0 to 3.01 × 10^{-7} mol J^{-1}; (2) G(e$_s^-$) decreases as [AgClO$_4$] increases, going from 4.31 × 10^{-7} to 1.34 × 10^{-7} mol J^{-1}; and (3) the total yield (G(Ag°) + G(e$_s^-$)) increases

marginally with [AgClO$_4$] increasing from 4.31×10^{-7} to 4.35×10^{-7} mol J^{-1}.

The only free parameter in the simulations is the rate constant for reaction 10. The value determined by stochastic simulations is $k_{10} = 2.8 \times 10^{13}$ M^{-1} s^{-1}. The ability of Ag$^+$ to act as a scavenger for e$^-$ is supported by the kinetic behavior of e$_s^-$ as a function of [AgClO$_4$], outlined in (Figure 4).
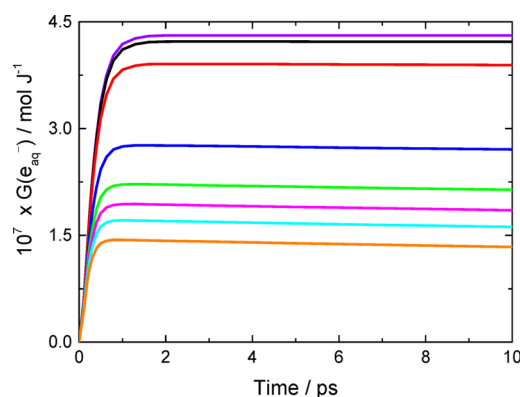

Figure 4. Radiolytic yield of e$_s^-$ as a function of time and AgClO$_4$ concentration; pure water (purple line), 0.002 (black line), 0.01 (red line), 0.05 (blue line), 0.08 (green line), 0.1 (pink line), 0.12 (light blue line), and 0.15 (orange line) mol L^{-1} AgClO$_4$.

The decay kinetics of e$_s^-$ within the 2−10 ps time regime is essentially independent of [AgClO$_4$], whereas its initial yield is drastically affected. This latter behavior is a consequence of the scavenging capacity of Ag$^+$ for e$^-$ progressively increasing with [AgClO$_4$], leading to more e$^-$ being consumed by Ag$^+$. Consequently, there is less e$^-$ available to undergo thermalization to yield e$_s^-$, leading to a significant decrease in the initial yield of e$_s^-$. Although Ag$^+$ does scavenge e$_s^-$, the rate constant for the associated reaction is close to diffusion controlled and is significantly lower than that for scavenging e$^-$. Very little bulk diffusion controlled reaction is expected on a picosecond time scale. Consequently within the 2−10 ps time regime, scavenging of e$_s^-$ accounts for less than 5% of the total yield of Ag$^\circ$, and the decay kinetics are relatively insensitive to the concentration of silver ions. The simulated track kinetics predict the C$_{37}$ value for silver ion at 1 ps to be 0.135 mol L^{-1}, which is very close to that found experimentally above at 10 ps (Figure S1 inset in the SI).

The evolution of the transient absorption was also recorded for solutions containing different concentrations of silver ion with a constant 14.6 mol L^{-1} concentration of phosphoric acid (Samples 6−10). The concentration of H$_3$O$^+$ in these viscous solutions is about 5.7 mol L^{-1}. As already reported, the presolvated electron and solvated electron are completely scavenged by H$_3$O$^+$ within the electron pulse.[24] Therefore, the solvated electron is not likely to be observed spectroscopically. The absorption now observed at 370 nm is due to both the silver atom and the phosphate radical. To determine the contribution of absorbance of the silver atom, the weak absorbance of the phosphate radical was measured in the absence of silver ion (Figure 2 bottom). The corresponding kinetics (Figure S2 in the SI) was then subtracted from the observed decay kinetics of the mixed solutions. Figure 5 shows that, after subtraction of the phosphate radical contribution, the initial amplitude of the absorbance at 370 nm is strongly dependent on the concentration of silver ions. The yield of
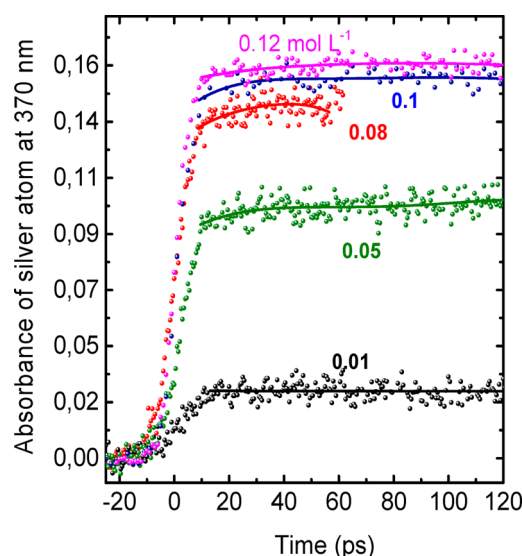

Figure 5. Kinetics observed at 370 nm in phosphoric acid solutions after subtraction of the absorption from the acid phosphoric radical H$_2$PO$_4^\bullet$.

silver atoms at the end of the pulse is high (ranging from 0.47×10^{-7} to 2.8×10^{-7} mol J^{-1}), and for the lower concentrations surprisingly even slightly higher than those found in neutral solution.

Phosphoric acid solutions are very viscous, and reactions controlled by diffusion are slow and do not occur in the first nanosecond. The radicals of phosphoric acid are formed via two mechanisms within 7 ps of the electron pulse: direct electron detachment and oxidation by the H$_2$O$^{\bullet+}$.[25] Recently, the time-resolved visible absorption spectra in three concentrated acid solutions (perchloric, sulfuric, and phosphoric) showed that, in contrast to previous reports, a strong blue shift of the absorption band of solvated electron in acidic solutions compared to neat water is clearly observed. This observation is consistent with the formation of a pair between the solvated electron and H$_3$O$^+$. Moreover, it was reported that the value of C$_{37}$ for scavenging of presolvated electron is around 3.5 mol L^{-1}. This value is much larger than those measured for other scavengers of presolvated electrons such as cadmium ion, nitrate, selenate, or bipyridine. The scavenging of the presolvated electron by H$_3$O$^+$ (reaction 11) in highly concentrated acid solutions has been previously reported by Gauduel et al.[26] It was proposed that an "ion pair", (H$_3$O$^+$, e$^-$), is formed between the presolvated electron and H$_3$O$^+$, exhibiting an absorption around 900 nm instead of around 1200 nm. This "ion pair" might be considered as the precursor to H$^\bullet$.

In the experiments reported here, the concentration of H$_3$O$^+$ in the phosphoric acid solutions is sufficiently high that scavenging of presolvated electrons by H$_3$O$^+$ should be very efficient. Consequently, a significant fraction of precursor to the solvated electron can be scavenged by H$_3$O$^+$. If we assume that the yield of the solvated electron is the same as initial yield of solvated electron in neutral water, i.e. it is around 4.2×10^{-7} mol J^{-1}, the C$_{37}$ value of silver ions in acidic medium is lower than 0.12 mol L^{-1}. This value is very low, suggesting that in acidic solutions the silver ion is one of the most powerful presolvated electron scavengers. To understand the formation of silver atom in acidic solutions the following points should be considered: (1) Phosphate ions do not react efficiently with

free electrons. (2) The hydration of free electrons will be considerably slower than in pure water due to the lower concentration of water in concentrated phosphoric acid solutions. (3) The yield of geminate recombination of electrons with $H_2O^{\bullet+}$ will be significantly reduced, as a significant fraction of $H_2O^{\bullet+}$ is replaced by phosphate radical which could be less effective at recombination reactions.

The only major reaction pathway left for the presolved electron is through scavenging by solutes present at low concentration. However, these reasons alone cannot explain the high yield of silver atom formed at short times in acidic solutions, except if we assume that the pair (e^-, H_3O^+) is capable of reducing silver ion within the irradiation pulse. This postulation would indicate that is whatever state the presolvated electron is, be it free or paired with H_3O^+, scavenging by silver ion (through reactions 10 and 13) is effective, meaning that the rate constant for reaction 13 should be close to that of reaction 10 suggested here by simulation.

CONCLUSION

In conclusion, the silver ion can be readily reduced in neutral solutions by the precursor of the solvated electron and even more spectacularly by the precursor of $H^\bullet$ in acidic solutions, (H_3O^+, e^-). The scavenging of precursor species by the silver ion is very efficient and even solutions with low concentrations of silver ion will result in this ultrafast reduction. Furthering our knowledge on the reactivity of short-lived species in irradiated water at ultrafast time scales is necessary to understand the competitive reactions occurring within the first few ps. The composition of aqueous solutions can potentially favor or inhibit one of these competitive ultrafast processes, such as electron hydration, electron hole recombination, or reduction of the solute. Consideration of the presented ultrafast reduction reactions can be crucial under certain conditions. For example, radiolytic methods are typically used for the synthesis of metal nanoparticles. As the dynamics of metal nanoparticle growth depends on certain atoms acting as nucleation sites (i.e., seeds for growth), it is important to know whether metal atoms, for example silver atoms, can be formed through the scavenging of key water radiolytic species even at low concentrations.

Finally, it is important to further develop the Monte Carlo radiation track structure simulations to accommodate systems in which the concentration of water is significantly lower than 55.4 mol L^{-1}, e.g. 14.6 mol L^{-1} H_3PO_4, in which the concentration of water is 14.1 mol L^{-1}.

ASSOCIATED CONTENT

Ⓢ Supporting Information

Description of the picosecond pulse radiolysis setup and three figures. The Supporting Information is available free of charge on the ACS Publications website at DOI: 10.1021/ acs.jpcb.5b04907.

AUTHOR INFORMATION

Corresponding Author

*E-mail: mehran.mostafavi@u-psud.fr. Tel: 33169157887.

Notes

The authors declare no competing financial interest.

ACKNOWLEDGMENTS

REFERENCES

(1) Haïssinsky, M. In *Radiation Chemistry*; Dobo, J., Hedwig, P., Eds.; Akad. Kiado: Budapest, 1972; Vol. 2, p 1353 and following discussion.

(2) Henglein, A. The Reactivity of Silver Atoms in Aqueous Solution (A Gamma -Radiolysis Study). *Ber. Bunsen-Ges. Phys.Chem.* **1977**, *81*, 556−561.

(3) Henglein, A. Reactions of Organic Free Radicals at Colloidal Silver in Aqueous Solution: Electron Pool Effect and Water Decomposition. *J. Phys. Chem.* **1979**, *83*, 2209−2216.

(4) Mostafavi, M.; Marignier, J.-L.; Amblard, J.; Belloni, J. Nucleation Dynamics of Silver Aggregates Simulation of Photographic Development Processes. *Radiat. Phys. Chem.* **1989**, *34*, 605−617.

(5) Janata, E.; Lilie, J.; Martin, M. Instrumentation of Kinetic Spectroscopy—11. An Apparatus for a.c.-Conductivity Measurements in Laser Flash Photolysis and Pulse Radiolysis Experiments. *Radiat. Phys. Chem.* **1994**, *43*, 353−356.

(6) Janata, E. Instrumentation of Kinetic Spectroscopy—12. Software for Data Acquisition in Kinetic Experiments. *Radiat. Phys. Chem.* **1994**, *44*, 449−454.

(7) Janata, E.; Henglein, A.; Ershov, J. The First Clusters of Ag^+ Reduction in Aqueous Solution. *J. Phys. Chem.* **1994**, *98*, 10888−10890.

(8) Remita, S.; Mostafavi, M.; Delcourt, M. O. Stabilization, Growth and Reactivity of Silver Aggregates Produced by Radiolysis in the Presence of EDTA. *New J. Chem.* **1994**, *18*, 581−588.

(9) Mostafavi, M.; Delcourt, M.-O.; Keghouche, N.; Picq, G. Early Steps of Formation of Silver/Polyacrylate Complexed Oligomer Clusters. A Pulse Radiolysis Study. *Radiat. Phys. Chem.* **1992**, *40*, 445.

(10) Belloni, J.; Mostafavi, M.; Remita, H.; Marignier, J.-L.; Delcourt, M.-O. Radiation-Induced Synthesis of Mono- And Multi-Metallic Clusters and Nanocolloids. *New J. Chem.* **1998**, *22*, 1239−1255.

(11) Khatouri, J., Mostafavi, M.; Belloni, J. Kinetics of Electron Transfer in Solution Catalyzed by Metal Cluster. In *Photochemistry and Radiation Chemistry*; Wishart, J., Nocera, D., Eds.; Adv. Chem. Ser.; American Chemical Society: Washington, DC, 1998; vol. 254, pp 293−314.

(12) Khatouri, J.; Mostafavi, M.; Amblard, J.; Belloni, J. Ionization Potential of Clusters in Liquid. *Z. Phys. D: At., Mol. Clusters* **1993**, *26*, 82−86.

(13) Buxton, G. V.; Greenstock, C. L.; Helman, W. P.; Ross, A. B.; Tsang, W. Critical Review of Rate Constants for Reactions of Hydrated Electrons, Hydrogen Atoms and Hydroxyl Radicals in Aqueous Solutions. *J. Phys. Chem. Ref. Data* **1988**, *17*, 513−886.

(14) Sarkar, A.; Janata, E. Formation of the Silver Hydride Ion AgH^+ Upon the Reduction of Silver Ions by $H^\bullet$ in Aqueous Solution. A Pulse Radiolysis Study. *Z. Z. Phys. Chem.* **2007**, *221*, 403−413.

(15) Aldrich, J. E.; Bronskill, M. J.; Wolff, R. K.; Hunt, J. W. Picosecond Pulse Radiolysis. III. Reaction Rates and Reduction in Yields of Hydrated Electrons. *J. Chem. Phys.* **1971**, *55*, 530−539.

(16) Jonah, C. D.; Miller, J. R.; Matheson, M. S. The Reaction of the Precursor of the Hydrated Electron with Electron Scavengers. *J. Phys. Chem.* **1977**, *81*, 1618−1622.

(17) Pimblott, S. M.; LaVerne, J. A. On the Radiation Chemical Kinetics of the Precursor to the Hydrated Electron. *J. Phys. Chem. A* **1998**, *102*, 2967−2975.

(18) Belloni, J.; Monard, H.; Gobert, F.; Larbre, J. P.; Demarque, A.; De Waele, V.; Lampre, I.; Marignier, J. L.; Mostafavi, M.; Bourdon, J. C.; et al. ELYSE A Picosecond Electron Accelerator for Pulse Radiolysis Research. Nucl. Instrum. Methods. *Nucl. Instrum. Methods Phys. Res., Sect. A* **2005**, *539*, 527−539.

(19) Marignier, J. L.; de Waele, V.; Monard, H.; Gobert, F.; Larbre, J. P.; Demarque, A.; Mostafavi, M.; Belloni, J. Time-Resolved Spectroscopy at the Picosecond Laser-Triggered Electron Accelerator ELYSE. *Radiat. Phys. Chem.* **2006**, *75*, 1024−1033.

(20) Schmidhammer, U.; Pernot, P.; De Waele, V.; Jeunesse, P.; Demarque, A.; Murata, S.; Mostafavi, M. Distance Dependence of the Reaction Rate for the Reduction of Metal Cations by Solvated Electrons: A Picosecond Pulse Radiolysis Study. *J. Phys. Chem. A* **2010**, *114*, 12042−12051.

(21) Janata, E.; Henglein, A.; Ershov, B. G. First Clusters of Ag^+ Ion Reduction in Aqueous Solutions. *J. Phys. Chem.* **1994**, *98*, 10888−10890.

(22) LaVerne, J. A.; Pimblott, S. M. New Mechanism for H_2 Formation in Water. *J. Phys. Chem. A* **2000**, *104*, 9820−9822.

(23) Pimblott, S. M.; LaVerne, J. A. Effects of Track Structure on the Ion Radiolysis of the Fricke Dosimeter. *J. Phys. Chem. A* **2002**, *106*, 9420−9427.

(24) Ma, J.; Schmidhammer, U.; Mostafavi, M. Direct Evidence for Transient Pair Formation between a Solvated Electron and H_3O^+ Observed by Picosecond Pulse Radiolysis. *J. Phys. Chem. Lett.* **2014**, *5*, 2219−2223.

(25) Ma, J.; Schmidhammer, U.; Mostafavi, M. Picosecond Pulse Radiolysis of Highly Concentrated Phosphoric Acid Solutions: Mechanism of Phosphate Radical Formation. *J. Phys. Chem. A* **2014**, *118*, 1−6.

(26) Gauduel, Y.; Pommeret, S.; Migus, A.; Antonetti, A. Some Evidence of Ultrafast H_2O^+ -Water Molecule Reaction in Femtosecond Photoionization of Pure Liquid Water. Influence on geminate Pair Recombination. *Chem. Phys.* **1990**, *149*, 1−10.